

Enhanced Photochemical Sensitivity in Photochromic Diarylethenes Based on a Benzothiophene/Thiophene Nonsymmetrical Structure

Olivier Galangau,^[a] Yuka Kimura,^[a] Rui Kanazawa,^[a] Takuya Nakashima,^[a] and Tsuyoshi Kawai*^[a]

Keywords: Photochromism / Noncovalent interactions / Density functional calculations / Diarylethenes

Photosensitivity of molecules is one of the central subjects of organic photochemistry. In this article, we present how and why a benzothiophene moiety impacts the photochromic quantum yield for the photochemical pericyclic ring closing of the hexatriene moiety. Two compounds were prepared: a symmetrical one incorporating two fluorenylthiophene units, and its corresponding nonsymmetrical partner, where one of the thiophene units was replaced by a benzothiophene

group. Interestingly, the latter presents relatively high cyclization quantum yield (0.74), a value close to the largest one so far reported. Based on crystal structures, VT-NMR data and DFT calculations, we demonstrate that introducing a benzothiophene in the molecular scaffold induces skeleton stiffening by means of CH- π interactions and steric repulsions, and leads to increased population of the reactive conformer in the ambient conditions.

Introduction

Diarylethenes (DAEs) and their aromatic analogues have been the subject of intense research over the past two decades. These classes of compounds undergo a reversible photochromic reaction between two stable forms: the ring-opened form with the hexatriene backbone and the ring-closed form with the cyclohexadiene backbone.^[1,2] Their high fatigue resistance and low thermal reactivity make these derivatives highly promising for optoelectronics applications.^[3–7] The photochemical parameter that governs the photocyclization sensitivity is well defined as the quantum yield $\Phi_{o/c}$. The quantum yield has been shown to predominantly depend on the ground state equilibrium between the nonreactive parallel and the reactive antiparallel conformers, because their ultrafast photo-excited state lifetimes of less than several picoseconds restrict rotational isomerization in the excited state.^[3] The photoisomerization serves as “snapshot” of the geometry of the open form in equilibrium with the reactive and the nonreactive conformations. Meanwhile, the contribution of a twisted intramolecular

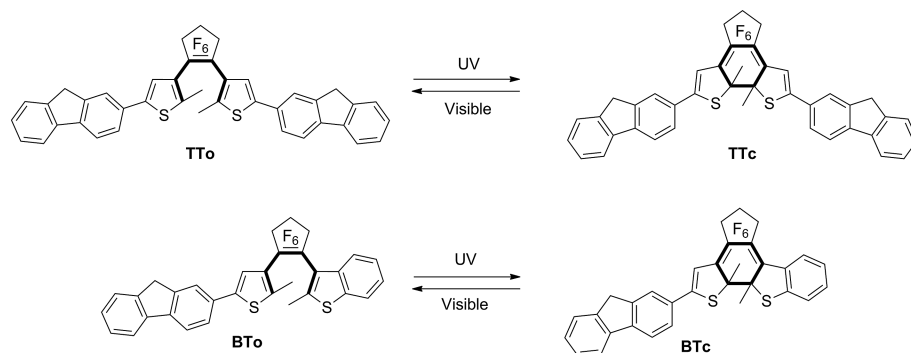
charge transfer (TICT) nature in the excited state is believed to suppress the ring cyclization reaction, which rises especially in standard DAEs with central ethene units bearing strong electron-withdrawing groups in polar environments.^[8] Some DAEs show $\Phi_{o/c}$ values close to unity in in single-crystalline samples.^[9] Amongst the several DAE-related substances displaying high $\Phi_{o/c}$ values in the solution phase,^[10] some, in which the DAE backbone was modified for stabilizing the reactive conformation with noncovalent attractive interactions between noncarbon atoms, have also displayed significant $\Phi_{o/c}$ values.^[11–16]

Since these approaches require fiddly and specific designs with limited choice of molecular structures, it is still worth studying the relationship between photoreactivity and molecular structure of the usual DAE backbone.

In the class of standard perfluoroDAEs (DAEs containing a perfluorocyclopentene central moiety), the highest $\Phi_{o/c}$ value so far reported (0.79) has been established for a structurally simple, nonsymmetrical compound featuring a benzothiophene moiety and a thiophene unit.^[17] A reference compound with symmetrical structure has denoted suppressed photoreactivity. Yet, no clarification has been provided to unveil the causes of such a $\Phi_{o/c}$ high value and the effect of its nonsymmetric backbone structure. This lack of systematic knowledge motivated us to synthesize two analogous compounds, **TT** and **BT**, and to study their structural and photophysical properties in condensed and solution phases (see Scheme 1).

[a] Graduate School of Materials Science, Nara Institute of Science and Technology, NAIST, 8916-5 Takayama-cho, Ikoma, Nara 630-0192, Nara, Japan
E-mail: tkawai@ms.naist.jp
<http://mswebs.naist.jp/LABs/kawai/english/>

Supporting information for this article is available on the WWW under <http://dx.doi.org/10.1002/ejoc.201402774>.



Scheme 1. Ring cyclization and ring cycloreversion photoreactions of **TT** (top) and **BT** (bottom) compounds.

Results and Discussion

Syntheses

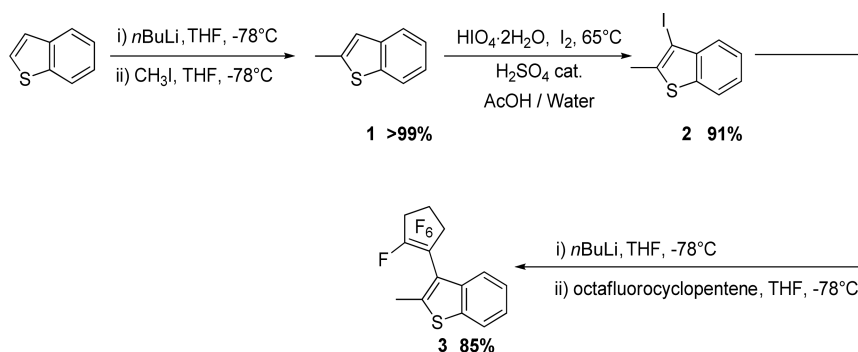
Our approach to synthesizing compounds **TT** and **BT** hinges on a final and flexible C–H organometallic arylation coupling between the central photochromic core compound **7** (or compound **6**) and the commercially available 2-iodofluorene.^[18] To this end, we first focused on preparing the corresponding intermediate derivatives **1–3** (Scheme 2).

Commercially available benzothiophene was successfully methylated at the α -position at low temperatures and then converted into the corresponding β -iodo derivative **2** using conventional strong iodination conditions.^[19] Finally, Li/I exchange at low temperatures and the subsequent nucleophilic substitution onto the perfluorocyclopentene eventually afforded precursor **3** in excellent yields.^[20] In the meantime, a “halogen dance” reaction^[21] on 2,5-dibromothiophene afforded **4** in excellent yield. Li/Br exchange followed by a substitution onto TMSCl or TiPSCl resulted in obtaining derivatives **5a** or **5b** in 72% yields. It must be noted that the both **3** and **5** were obtained with an overall yield of 77% and 60%, respectively, on a scale of up to several grams. Final coupling between compounds **3** and **5** through Li/Br exchanges followed by nucleophilic substitutions onto compound **3** led to the targeted intermediate **6** in good yield. Compound **7** was obtained from a standard nucleophilic substitution onto the commercially available perfluorocyclopentene (Scheme 3).

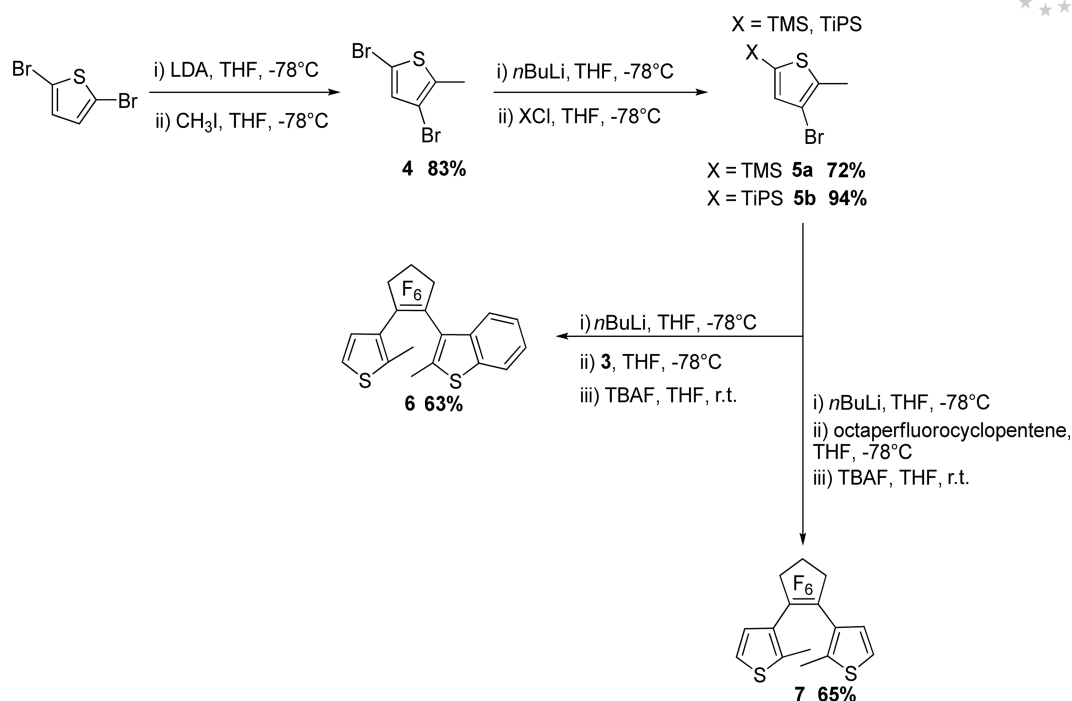
Compounds **TT** and **BT** were prepared in moderate yields according to a reported procedure of CH direct arylation developed by Shinokubo et al., using the strong reactivity of the thiophene’s α -proton (Scheme 4). The ¹H NMR spectrum (see Supporting Information) displaying a singlet signal located in the aromatic region ($\delta = 7.18$ ppm for **BT** and $\delta = 7.33$ ppm for **TT** in CDCl₃) and X-ray data (see X-ray discussion) are consistent with the presence of a hydrogen atom placed on the thiophene’s β position.

Photophysical Studies

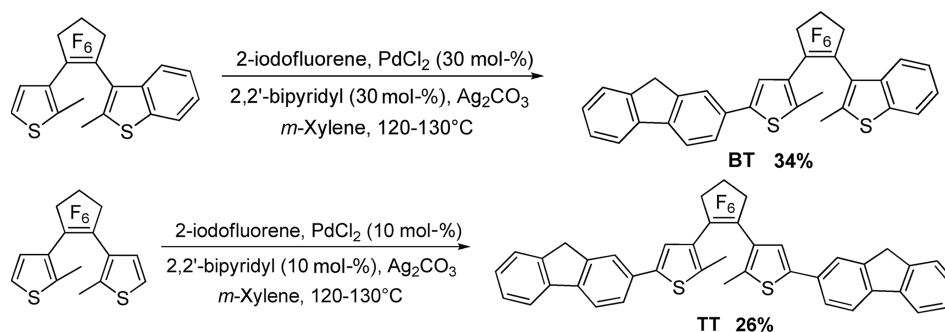
The spectrophotometric properties of both compounds were investigated in toluene. Their open form isomers, namely **TTo** and **BTo**, feature absorption maxima located in the UV part of the optical absorption spectra (Table 1). Under UV light irradiation at 313 nm, both absorption spectra undergo deep variations, testifying of the emergence of new bands safely assigned to the corresponding closed-form isomers **TTc** and **BTc** (Figure 1 and Scheme 1). As the photoreaction proceeds, the spectra display isosbestic points located at 355 nm and 354 nm, suggesting two-component photoisomerizations. Visible light irradiation (> 500 nm) drives the cycloreversion reaction with the same isosbestic points and allows a full recovery of the starting open form spectra. These phototransformations can be done repetitively without signs of any degradation, although some occurred under prolonged 254 nm irradiation.



Scheme 2. Synthesis of compounds **1–3**.



Scheme 3. Syntheses of compounds 4–7.

Scheme 4. Syntheses of compounds **TT** and **BT**.

tions. The photocyclizations were monitored by ^1H NMR in $[\text{D}_8]$ toluene to assess their conversion (see Supporting Information) and were evaluated to be 0.94 for both derivatives.

Table 1. Photophysical properties of **TT** and **BT** derivatives in toluene. Solutions were not degassed.

	λ_{max} [nm]	ϵ (λ_{max}) [L mol $^{-1}$ cm $^{-1}$]	$\Phi_{\text{oc}}^{\text{[a]}}$	$\Phi_{\text{cl}}^{\text{[b]}}$	χ
TTo	332	79500 \pm 100	0.62 \pm 0.01	–	0.94
TTc	610	25100 \pm 100 ^[c]	–	0.0013	–
BTo	327	35200 \pm 100	0.74 \pm 0.01	–	0.94
BTc	562	19300 \pm 100 ^[c]	–	0.022	–

[a] Reported as absolute values at 313 nm. [b] Reported as absolute values at 510 nm. [c] Closed form isomers were separated by reversed-phase HPLC.

Both open-form compounds absorb in a similar wavelength range, with a maximum of absorption slight red-shifted by 5 nm for **TTo**. Interestingly, replacing one fluorenylthiophene with a benzothiophene reduces drastically

the extinction coefficient. We also measured the ring cyclization quantum yield for the both compounds. While **TTo** shows a classical value of 0.62 as observed for symmetrical DAEs,^[22] **BTo** displays a higher value of 0.74, close to the highest ring cyclization quantum yield so far reported. On these bases, we investigated the conformational equilibria of **TTo** and **BTo** by Variable Temperature ^1H NMR (VT-NMR) in order to determine whether or not these values originate from a conformational issue.

Following the seminal work of Coudret et al.^[23] and assuming a fast equilibrium between an *antiparallel* (photo-reactive) and a *parallel* (non-reactive) conformers, we evaluated the population ratio of antiparallel conformer at 293 K. We monitored as a function of the probe's temperature the methyl signals chemical shifts (Figure 2, Table 2 and Supporting Information).

For both compounds, no signal splitting was observed, meaning that the fast equilibrium still took place even at the low temperatures. Due to the symmetrical nature of **TTo**, a sole singlet signal was subjected to a large shift of 0.35 ppm

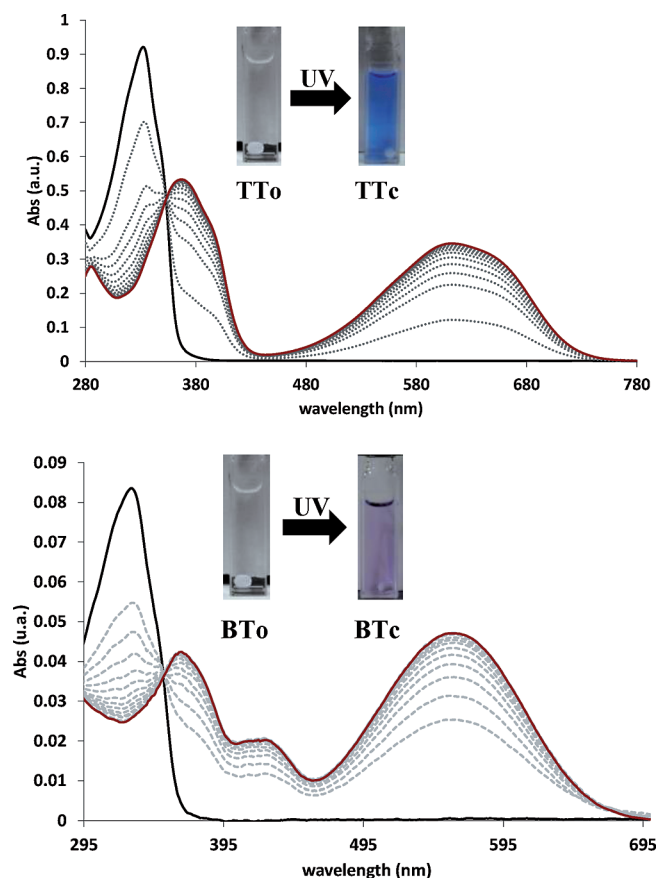


Figure 1. UV/Vis monitoring of the ring cyclization processes of **TTo** (top) and **BTo** (bottom). Black curve: open forms, red curve: photostationary state.

upon raising the temperature. Estimation of the antiparallel population ratio gave a 65% value, which is consistent with the ring cyclization quantum yield observed. For **BTo**, the signals of two methyl groups were monitored as functions of the probe temperature. The methyl attached to the thiophene ring was subjected to a downfield shift of 0.48 ppm upon heating, while the signal of the methyl group on the benzothiophene moiety shifted by 0.30 ppm from 193 K to 313 K. These outcomes suggest that the magnetic environment of the methyl group attached to the thiophene ring changed in more pronounced way than for the other methyl group during the interconversion. Moreover, the antiparallel population at 293 K was determined to be approximately 70%, a value consistent with the measured quantum yield. Standard Gibbs free energy differences between the conformations can also be roughly estimated and were calculated to be 0.40 kcal mol⁻¹ for **TTo** and 0.60 kcal mol⁻¹ for **BTo** (average value). Although the equilibria are likely to be disfavoured in both situation, the benzothiophene core hampers even more the conformational change. The cycloreversion quantum yields of the compounds follow the well-established tendency that the DAEs with longer π -conjugation system exhibit lower cycloreversion reactivity.^[24]

These results suggest that the ring cyclization quantum yields are strictly limited by the relative population of reac-

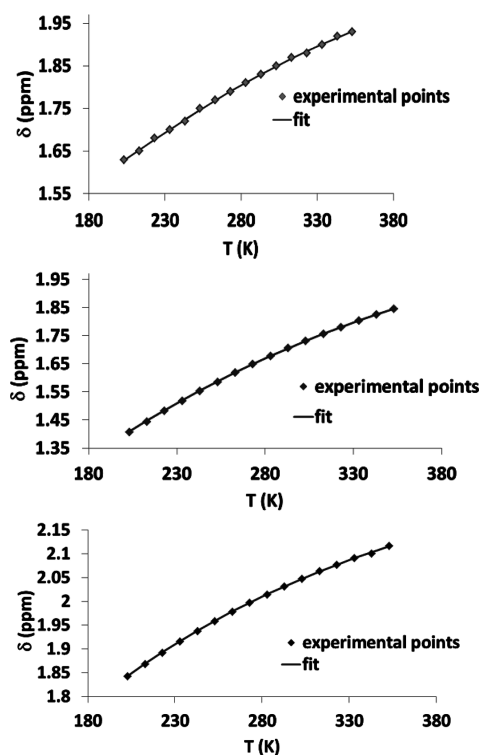


Figure 2. ¹H NMR monitoring of the methyl group's chemical shifts as functions of probe temperature for **TTo** (top), **BTo**-benzothiophene signal (middle) and **BTo**-thiophene signal (bottom).

Table 2. VT-NMR spectroscopic data for compounds **TTo** and **BTo**.

	$\Delta\delta$ [ppm]	ΔG^0 [kcal mol ⁻¹]	Population of anti-parallel isomers
TTo	0.35	0.40	65 ± 5%
BTo			
CH ₃ ,thiophene	0.48	0.70	71 ± 8%
CH ₃ ,benzothiophene	0.30	0.50	70 ± 6%

tive conformer in the media and not by photodynamic processes such as contribution of TICT states. Inserting one benzothiophene moiety instead of a thiophene ring, though, results in more energetically demanding conformational change, probably originating from an efficient stabilization of the reactive conformer. On those bases, we investigated the solid-state structures of **TTo** and **BTo**.

Crystal Structures

Crystals of compounds **TTo**^[25] and **BTo**^[26] were obtained by slow evaporation of solvents from toluene solutions. **TTo** crystallized into a triclinic system [*P* $\bar{1}$ (#2) space group] while **BTo** crystallized into an orthorhombic system [*Pbca* (#61) space group] (Figure 3). Both derivatives crystallized into the photoreactive antiparallel conformation. The two reactive carbon centers are 3.56 Å apart for **TTo** and 3.89 Å apart for **BTo**, which are shorter distances than the typical limiting photoreactivity distance in the crystal state of 4.2 Å.^[27]

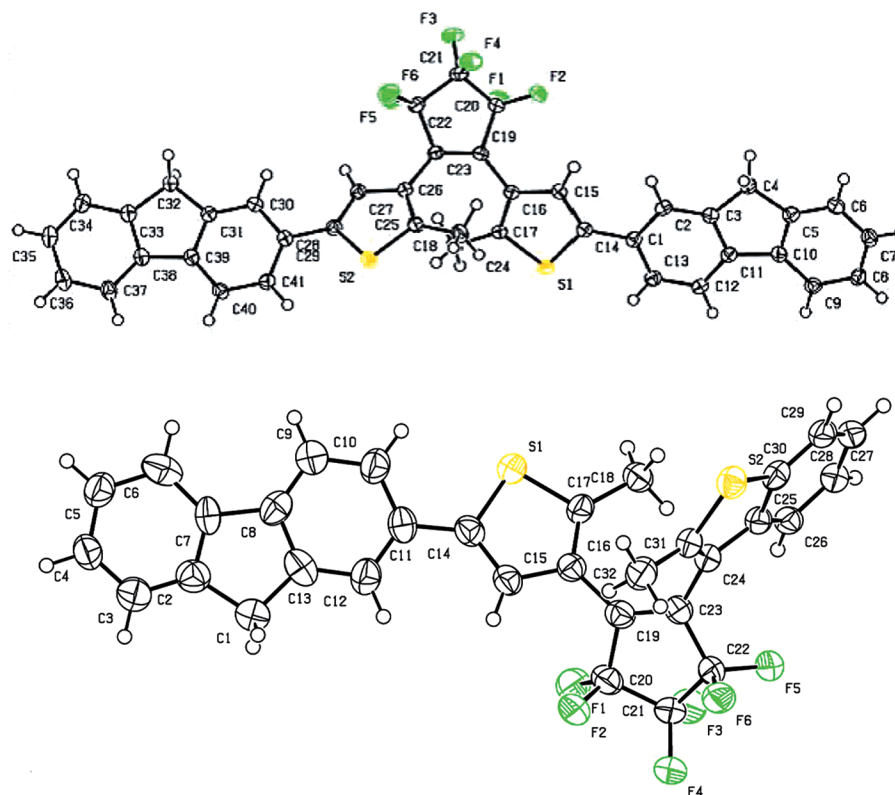


Figure 3. Crystal structures of **TTo** (top) and **BTo** (bottom).

Both crystals have presented photochromic properties (not shown). The **TTo** crystal structure featured torsion angle values around 43° (see Supporting Information) between the side aryl units and the central bridge unit, reflecting the molecule's symmetrical nature. On the other hand, **BTo**'s structure showed a marked difference in the torsion angles. Indeed, while the torsion angle between the thiophene and the bridge is 45° , similar to **TTo**, the benzothiophene and the bridge form a large torsion angle of 66° . Both crystals feature intramolecular noncovalent interactions, which are believed to stabilize their reactive conformations. One should note that the distances between the fluorine atoms of the bridge and the β -hydrogen of the thiophenes are shorter than the sum of their Van der Waals radii ($r_H = 1.20 \text{ \AA}$ and $r_F = 1.47 \text{ \AA}$). For example, **TTo** showed slightly different distance values of 2.41 \AA and 2.55 \AA , signifying strong hydrogen bonds in both sides of the molecule, which helps to maintain the conformation into the antiparallel orientation. Although, **BTo** showed a significantly larger distance of 2.63 \AA , it suggests that this interaction must be weak, but still exists. In addition, 1D ^{19}F NMR experiments were carried out to confirm the existence of these CH–F interactions in solution (see Supporting Information). For both molecules, signal broadening was observed at 20°C when decoupling protons from fluorine atoms, clearly indicating H–F interactions, especially in **BTo**. Moreover, the two X-ray structures display very clear CH– π interactions occurring between hydrogen atoms of the methyl groups and the opposite heteroaromatic rings.

In the case of **TTo**, for example, the distances in the both sides (see Supporting Information) were evaluated to be 2.83 \AA and 2.75 \AA . These values are consistent with typical CH– π interaction distances.^[28] This also suggests that a third interaction contributes to maintaining the molecular scaffold in the antiparallel conformation. However, **BTo** shows a completely different feature. Because the benzothiophene moiety has a large torsion angle with respect to the central bridge, the distance between the methyl group on the thiophene unit and the π -system on the benzothiophene core is 2.76 \AA , which allows a CH– π interaction for only one of the methyl groups. Consequently, the symmetry breaking on the hexatriene backbone results in a strong and mono-directional CH– π interaction, resulting in a highly sterically constrained structure (space filling views, see the Supporting Information) in which the benzothiophene core is sandwiched between the perfluoro-bridge on one side and the methyl thiophene on the other. As opposed to **TTo**, **BTo**'s interactions seem to strongly rigidify the molecular scaffold, and should impact on the photochromic properties in solution.

All together, these data suggest that the replacement of one side group of **TT** by a benzothiophene unit induces a large conformational change in the crystal structure. It also brings the emergence of intramolecular interactions of various natures (F–H bonds, CH– π interactions, steric repulsions) that stabilize the antiparallel conformation, and results in a loss of molecular flexibility. Although, solute–solvent interactions are important, these crystal properties

FULL PAPER

only partly explain the observed conformational differences between the two derivatives in the solution phase.

DFT and TD-DFT Calculations

We also performed calculations on **TTo**/**TTc** and on **BTo**/**BTc** to gain a better insight into their electronic properties. Optimizations were carried out at the B1B95 6-311g (d,p) level of theory, which is known to provide the best compromise between the geometrical minimization and theoretical UV spectra.^[29] Simulations of IR spectra were also performed to make sure that optimization outcomes corresponded to true minima. Finally, TD-DFT calculations were performed at the same level of theory. From the structural point of view, calculated structures of **TTo** and **BTo** match the experimental ones (Table 3) with reasonable deviation.

Table 3. Comparison of the structural parameters obtained by DFT (calcd.) and by X-ray diffraction (exp).

	T_{calc} [°]	T_{exp} [°]	$d_{\text{H-F calcd.}}$ [Å]	$d_{\text{H-F exp.}}$ [Å]	$d_{\text{CH-}\pi \text{ calcd.}}$ [Å]	$d_{\text{CH-}\pi \text{ exp.}}$ [Å]
TTo	44	47	2.49	2.41	2.72	2.75
	43	43	2.58	2.55	2.81	2.83
BTo	42	45	2.46	2.63	2.73	2.76
	57	66	–	–	–	–

As expected, DFT optimization provided a reliable model of these two derivatives. In particular, this method predicted the appearance of CH– π interactions^[30] as well as a strong steric hindrance between the perfluoro group and the benzothiophene moiety. The two corresponding closed forms, namely **TTc** and **BTc**, displayed similar flat structures, typical of these compounds.

TD-DFT and molecular orbitals (see Supporting Information) also provided us interesting information. In both compounds in their open forms, the LUMO orbital contributed to the photocyclization reaction, presenting the adequate bonding interaction between the two carbon centers in the excited state. While the HOMO in **TTo** extends to the two fluorenylthiophene moieties, that of **BTo** is more localized onto the fluorenylthiophene unit. In both systems, the HOMO to LUMO transition is accompanied by an electron density transfer from the side units to the center of the molecule, illustrating their weak charge transfer nature. The HOMO–LUMO transition of **BTo** exhibited a significant charge-transfer (CT) nature, which originated from its non-symmetrical molecular structure. The CT nature in the excited states of π -conjugated substances generally tends to stabilize the twisted excited state (TICT) and thus the CT nature in the DAE backbone has been thought to suppress the photocyclization reactivity.^[8b–8c] The present opposite tendency in the photoreactivity suggests that the photoreactivity in **TTo** and **BTo** is dominated by the ground state geometry but not by the excited state electronic structures in nonpolar solvents.^[31] The HOMO–LUMO gap was rather unaffected when the thiophene was replaced by a benzothiophene unit, as seen in the small difference be-

tween the HOMO–LUMO gaps (4.26 eV for **TTo**, 4.31 eV for **BTo**). However, introducing a benzothiophene drastically diminished the oscillating strength by more than a factor 2, which is consistent with the observed variation of extinction coefficient values ($S_0 \rightarrow S_3$, $f = 2.1$ for **TTo**, $f = 0.9$ for **BTo**). On the contrary, the molecular orbitals of the corresponding closed forms **TTc** and **BTc** were distributed similarly over the two molecules. As commonly noticed for the closed forms of DAEs, the lowest energy transition was assigned to the HOMO–LUMO transition. Compared to **TTc**, **BTc** showed a large blueshift of 66 nm, induced by the loss of a fluorene moiety. Indeed, introducing a benzothiophene decreased the HOMO level, while the energy of the LUMO was barely affected (see Supporting Information). These calculations provided a good insight into the electronic properties of **TT** and **BT** compounds. They also predicted in both open forms the existence of stabilizing intramolecular interactions (CH– π , H–F bonding).

Conclusions

We have designed two new push–pull DAEs, namely **BT** and **TT** derivatives, and studied their structural and photo-physical properties in solution, as well as in the solid state. Both compounds exhibited photochromic reactions in solution and condensed phases. The highest ring cyclization quantum yield in solution was obtained for compound **BT**, in which strong CH– π interactions and H–F bonding interactions were involved, as shown by X-ray, VT-NMR and ¹⁹F NMR data. Combined with the loss of molecular flexibility, the intramolecular interactions must drive the molecular conformation toward the most reactive one, and therefore must enhance the photocyclization efficiency. Solvent polarity might also impact the equilibria by destabilizing the parallel conformer, consistent with the slight enhancement of $\Phi_{o/c}$ we observed in the case of **BTo**. Nonetheless, several groups reported that for compounds analogous to **BT**, various efficiencies as functions of the nature of the aromatic groups connected to the thiophene ring, hence highlighting its key role.^[32] We are now focusing our research efforts on studying the influence of this aromatic ring nature upon the overall ring cyclization quantum yield.

Experimental Section

General: Chemicals were purchased from Tokyo Chemical Industries, Wako Chemicals and Sigma Aldrich, and were used without any further treatment. Dry solvents were purchased from Nacalai Tesque and Sigma Aldrich, and were kept under nitrogen atmosphere. Spectroscopic grade solvents were purchased from Wako chemicals. ¹H and ¹³C NMR spectrum were recorded with JEOL JNM-AL-300 (300 MHz) and JEOL JNM-ECP400 (400 MHz) spectrometers. Chemical shifts were referenced to the solvent residue peaks. Mass spectra were measured with a JEOL AccuTOF JMS-T100LC (ESI) and JML-700 (EI) instruments. ATR-IR spectra were recorded with a JASCO FT/IR-4200 spectrometer with ATR PRO410-S. Melting points were measured with a capillary MEL-TEMP apparatus and are not corrected. Purifications by

automatic column chromatography were performed on a YAM-AZEN W-Prep 2XY system. Compounds that were studied by spectroscopic measurement of any kind were first purified by HPLC using 8391 NEXT HPLC from Japan Analysis Industry. Separations of open- and closed-form isomers were carried out on a HITACHI LaChrom ELITE Reversed Phase HPLC system.

Photophysical Studies: Absorption spectra were recorded with a UV-Vis spectrophotometer (JASCO V-670 or V-660). Absolute ring cyclization quantum yield values were obtained with a Shimadzu QYM-01 setup. Prior to the photophysical experiments, samples were subjected to GPC purification and were evaporated under high vacuum in the dark during almost a week. Light intensities were evaluated by using CUSTOM UV 340 and ADVANTES Q8221 as power meters, for UV and visible irradiations, respectively.

Synthetic Procedures: Compounds **1**, **2**, **3**, **4** and **5a** were synthesized according reported procedures.^[18,19]

(4-Bromo-5-methylthiophen-2-yl)triisopropylsilane (5b): A Schlenk tube equipped with a magnetic stirring bar and capped with a rubber septum was charged with 3,5-dibromo-2-methylthiophene (4.0 g, 16.0 mmol, 1 equiv.) followed by the addition of dry THF (80 mL). The solution was cooled to -78°C . At that temperature, a hexane solution of *n*BuLi (1.6 M, 9.8 mL, 17.2 mmol, 1.1 equiv.) was added dropwise with stirring. After 1 h at low temperature, neat chlorotriisopropylsilane was added dropwise (2.8 mL, 23.5 mmol, 1.5 equiv.), and the mixture was slowly warmed to room temperature. The reaction was quenched by carefully adding water, followed by an extraction with Et_2O . The organics were combined, dried with anhydrous magnesium sulfate and filtered, and the solvents were removed under reduced pressure. The crude material was subjected to silica gel column chromatography using hexane as the eluent. Purification afforded white crystals (4.87 g, 94% yield) with satisfactory purity. ^1H NMR (300 MHz, CDCl_3): δ = 1.08–1.10 (m, 18 H), 1.29 (m, 3 H), 2.43 (s, 3 H), 7.02 (s, 1 H) ppm. ^{13}C NMR (75 MHz, CDCl_3): δ = 11.6, 14.7, 18.5, 110.5, 131.7, 137.7, 139.3 ppm, m.p. 50°C . IR: $\tilde{\nu}$ = 749, 921, 1139, 1157, 1168, 1194, 1208, 1229, 1306, 1334, 1365, 1381, 1419, 1507, 1524, 1542, 1633, 1732, 2889 cm^{-1} . HRMS-EI: calculated for $\text{C}_{14}\text{H}_{25}\text{BrSSi}$ 332.0630; found 332.0622 [M^+].

3-[3,3,4,4,5,5-Hexafluoro-2-(2-methylthiophen-3-yl)cyclopent-1-enyl]-2-methylbenzo[*b*]thiophene (6): A two-necked round-bottomed flask equipped with a magnetic stirring bar and capped with a rubber septum was charged with compound **5** (2.0 g, 8.0 mmol, 1 equiv.). The flask was degassed and backfilled with argon several times. Dry THF (80 mL) was added, and the solution was cooled to -78°C using a dry ice/acetone bath. A hexane solution of *n*BuLi (1.6 M, 5.5 mL, 8.8 mmol, 1.1 equiv.) was added dropwise with stirring. After 45 min at -78°C , a THF (dry) solution of compound **3** (3.0 g, 8.8 mmol, 1.1 equiv.) was added. After stirring at -78°C for 1 h, a THF solution of TBAF (1 M, 9.6 mL, 9.6 mmol, 1.2 equiv.) was added dropwise, and the mixture was warmed to room temp. overnight. Water was carefully added to quench the reaction, and diethyl ether was added to extract the product. The organic layer was washed with brine, dried with anhydrous MgSO_4 , and the solids were filtered off. The filtrate was concentrated under reduced pressure. The crude product was purified by a chromatography on a silica gel column, using hexane as the eluent, to afford a white solid (2.34 g, 63% yield). ^1H NMR (300 MHz, CDCl_3): δ = 1.95 (s, 3 H), 2.25 (s, 3 H), 6.96 (d, J = 6 Hz, 1 H), 7.04 (d, J = 6 Hz, 1 H), 7.30–7.36 (m, 2 H), 7.53–7.56 (m, 1 H), 7.71–7.74 (m, 1 H) ppm. ^{13}C NMR (75 MHz, CDCl_3): δ = 14.5, 14.7, 120.3, 122.0, 122.1, 122.2, 123.3, 124.2, 124.4, 124.9, 125.1, 126.8, 127.1,

127.4, 138.2, 142.1, 142.4 ppm, m.p. $55\text{--}60^{\circ}\text{C}$. IR: $\tilde{\nu}$ = 500, 536, 571, 814, 840, 887, 938, 965, 984, 1021, 1040, 1051, 1097, 1111, 1133, 1150, 1187, 1200, 1251, 1296, 1290, 1334, 1356, 1432, 1442, 1534, 1622, 1654, 2323, 2343, 2855, 2946 cm^{-1} . HRMS-EI: calculated for $\text{C}_{19}\text{H}_{12}\text{F}_6\text{S}_2$ 418.0285; found 418.0289 [M^+].

3-{2-[2-Ethyl-5-(9*H*-fluoren-2-yl)thiophen-3-yl]-3,3,4,4,5,5-hexafluorocyclopent-1-enyl}-2-methylbenzo[*b*]thiophene (BTo): A two-necked round-bottomed flask equipped with a magnetic stirring bar, a refluxed condenser and capped with a rubber septum was charged with PdCl_2 (38 mg, 30 mol-%) and 2,2'-bipyridyl (34 mg, 30 mol-%). The flask was evacuated and backfilled with argon several times. Dry *m*-xylene (1.2 mL) was added, and the mixture was stirred at 60°C (bath temperature) over a period of 40 min. Then, compound **6** (300 mg, 0.7 mmol, 1 equiv.), 2-iodofluorene (629 mg, 2.2 mmol, 3.0 equiv.) and Ag_2CO_3 (297 mg, 1.1 mmol, 1.5 equiv.) were added under argon. Dry *m*-xylene (1.2 mL) was added, and the mixture was heated at 130°C overnight. The mixture was cooled to room temp., and CH_2Cl_2 was added to dilute the mixture. The solution was filtered through a pad of silica to remove the remaining solids. The filtrate was concentrated under reduced pressure and purified by an automatic chromatography column, using silica gel and a mixture of hexane and CHCl_3 as eluent, affording a white solid (150 mg, 34% yield). ^1H NMR (300 MHz, CDCl_3): δ = 1.91 (s, 3 H), 2.29 (s, 3 H), 3.82 (s, 2 H), 7.18–7.71 (m, 12 H) ppm. ^{13}C NMR (75 MHz, CDCl_3): δ = 14.7, 14.8, 36.8, 119.9, 120.2, 120.3, 122.0, 122.1, 124.3, 124.5, 124.9, 125.0, 125.1, 126.8, 126.9, 131.6, 138.2, 141.0, 141.4, 141.5, 142.3, 142.5, 143.3, 143.9 ppm, m.p. $140\text{--}145^{\circ}\text{C}$. IR: $\tilde{\nu}$ = 607, 688, 849, 1071, 1207, 1294, 2847, 2900 cm^{-1} . HRMS-EI: calculated for $\text{C}_{32}\text{H}_{20}\text{F}_6\text{S}_2$ 582.0911; found 582.0909 [M^+].

3,3'-(Perfluorocyclopent-1-ene-1,2-diyl)bis(2-methylthiophene) (8): A flame-dried Schlenk tube equipped with a magnetic stirring bar was charged with (4-bromo-5-methylthiophen-2-yl)triisopropylsilane (4 g, 12 mmol, 2.2 equiv.) under a flux of nitrogen before dry THF (30 mL) was added. The solution was cooled to -78°C before a hexane solution of *n*BuLi (1.6 M, 7.5 mL, 12 mmol, 2.2 equiv.) was added dropwise with stirring. Stirring was maintained over 1 h at low temperature, then perfluorocyclopentene was quickly added (733 μL , 5.5 mmol, 1.0 equiv.), and the mixture was allowed to slowly warm to room temperature. Finally, a TBAF solution in THF (1 M, 13.7 mL, 14 mmol, 2.5 equiv.) was added dropwise. The reaction was quenched by addition of water. The biphasic system was extracted by adding Et_2O . The organics were washed several times with water, dried with anhydrous magnesium sulfate, filtered, and the solvents were evaporated under reduced pressure. The crude product was purified by a silica column chromatography using hexane as eluent, to afford transparent crystals (1.31 g, 65% yield) with satisfactory sample purity. ^1H NMR (300 MHz, CDCl_3): δ = 1.87 (s, 6 H), 7.07 (d, J = 6.0 Hz, 4 H), 7.16 (d, J = 6.0 Hz, 4 H) ppm. ^{13}C NMR (75 MHz, CDCl_3): δ = 14.1, 123.6, 124.9, 127.1, 141.7 ppm, m.p. 64°C . IR: $\tilde{\nu}$ = 603, 628, 637, 649, 664, 694, 713, 741, 804, 824, 843, 886, 893, 925, 981, 1042, 1055, 1104, 1155, 1190, 1203, 1268, 1336, 1362, 1380, 1436, 1542, 1635, 2854, 2924, 2957 cm^{-1} . HRMS-EI: calculated for $\text{C}_{15}\text{H}_{10}\text{F}_6\text{S}_2$ 368.0128; found 368.0149 [M^+].

3,3'-(Perfluorocyclopent-1-ene-1,2-diyl)bis[5-(9*H*-fluoren-2-yl)-2-methylthiophene] (TTo): A flame-dried Schlenk tube equipped with a magnetic stirring bar was charged with PdCl_2 (10 mg, 10 mol-%), 2,2'-bipyridyl (8 mg, 30 mol-%). The flask was evacuated and backfilled with argon several times. Dry *m*-xylene (0.9 mL) was added, and the mixture was stirred at $60\text{--}70^{\circ}\text{C}$ (bath temperature) over a period of 60 min. Then, 3,3'-(perfluorocyclopent-1-ene-1,2-

FULL PAPER

diyl)bis(2-methylthiophene) (200 mg, 0.5 mmol, 1 equiv.), 2-iodofluorene (476 mg, 1.6 mmol, 3.0 equiv.) and Ag_2CO_3 (450 mg, 1.6 mmol, 3 equiv.) were added under argon. Dry *m*-xylene (0.9 mL) was added, and the mixture was heated at 120–130 °C for 24 h. The mixture was cooled to room temp., and CH_2Cl_2 was added to dilute the mixture. The solution was filtered through a pad of silica to remove the remaining solids. The filtrate was concentrated under reduced pressure and purified by an automatic chromatography column, using silica gel and a mixture of hexane and CHCl_3 as eluent, affording a pale yellow solid (100 mg, 26% yield). ^1H NMR (300 MHz, CDCl_3): δ = 1.99 (s, 6 H), 3.94 (s, 4 H), 7.30–7.81 (m, 16 H) ppm. ^{13}C NMR (75 MHz, CDCl_3): δ = 14.6, 36.7, 120.0, 120.3, 122.0, 122.1, 124.5, 125.1, 125.9, 126.9, 127.0, 131.7, 141.0, 141.6, 142.7, 143.4, 144.0 ppm, m.p. 240 °C. IR: $\tilde{\nu}$ = 531, 563, 677, 732, 766, 823, 980, 995, 1058, 1108, 1192, 1263, 1340, 1429, 1449, 2850, 2965, 3050 cm^{-1} . HRMS-EI: calculated for $\text{C}_{41}\text{H}_{26}\text{F}_6\text{S}_2$ 696.1380; found 696.1364 [M^+].

Supporting Information (see footnote on the first page of this article): Copies of ^1H NMR and ^{13}C NMR spectra, VT-NMR spectroscopic data, NMR monitoring of the photoreaction, DFT calculations details, X-ray structural data.

Acknowledgments

O. G. thanks the Japan Society for the Promotion of Science and the Centre National pour la Recherche Scientifique (CNRS) for financial support. This work was also partly supported by the Ministry of Education, Culture, Sports, Science and Technology (MEXT), Japan (Grant-in-Aid for Scientific Research on Innovative Area, “Application of Cooperative Excitation into Innovative Molecular Systems with High-Order Photofunctions”) by the Nanotechnology Platform Program running in Japan Advanced Institute of Science and Technology, JAIST). The authors are grateful to Mr. M. Asanoma and Mr. M. Katao, technical staff members at NAIST, for their help with VT-NMR experiments and X-ray characterizations, respectively. Finally, the authors show their gratitude to Prof. Delbaere, Prof. Maurel, Dr. Sliwa, Dr. Aloïse and Dr. Perrier for fruitful discussions.

- [1] G. H. Brown (Ed.), *Photochromism, Techniques in Chemistry*, vol. 3, Wiley-Interscience, New York, NY, 1971.
- [2] H. Dürr, H. Bouas-Laurent (Eds.), *Photochromism: Molecules and Systems*, Elsevier, Amsterdam, 1990.
- [3] M. Irie, *Chem. Rev.* **2000**, *100*, 1684–1716.
- [4] B. L. Feringa, R. A. van Delden, N. Koumura, E. M. Geertsema, *Chem. Rev.* **2000**, *100*, 1789–1816.
- [5] V. Balzani, A. Credi, M. Venturi, in: *Molecular Devices and Machines: A Journey into the Nano World*, Wiley-VCH, Weinheim, Germany, 2003.
- [6] J. A. Delaire, K. Nakatani, *Chem. Rev.* **2000**, *100*, 1817–1816.
- [7] Y. Hasegawa, T. Nakagawa, T. Kawai, *Coord. Chem. Rev.* **2010**, *254*, 2643–2651.
- [8] a) S. Nakamura, T. Kobayashi, A. Takata, K. Uchida, Y. Asano, A. Murakami, A. Goldberg, D. Guillaumont, S. Yokojima, S. Kobatake, M. Irie, *J. Phys. Org. Chem.* **2007**, *20*, 821–829; b) M. Irie, K. Sayo, *J. Phys. Chem.* **1992**, *96*, 7671–7674; c) H. Miyasaka, T. Nobuto, M. Murakami, A. Itaya, N. Tamai, M. Irie, *J. Phys. Chem. A* **2002**, *106*, 8096–8102; d) M. Irie, M. Mohri, *J. Org. Chem.* **1988**, *53*, 803–808; e) S. Castellanos, L. Brubert, R. Stöber, S. Hecht, *J. Phys. Chem. C* **2013**, *117*, 23529–23538.
- [9] a) M. Irie, *Proc. Jpn. Acad., Ser. B* **2010**, *86*, 472–483; b) T. Yamada, S. Muto, S. Kobatake, M. Irie, *J. Org. Chem.* **2001**, *66*, 6164–6168; c) M. Irie, T. Lifka, S. Kobatake, N. Kato, *J. Am. Chem. Soc.* **2000**, *122*, 4871–4876; d) K. Shibata, K. Muto,

- S. Kobatake, M. Irie, *J. Phys. Chem. A* **2002**, *106*, 209–214; e) H. Wang, H. Lin, W. Xu, D. Zhu, *Chem. Eur. J.* **2013**, *19*, 3366–3373; f) T. Yamaguchi, W. Taniguchi, T. Kagawa, Y. Kamihashi, T. Ozeki, M. Morimoto, M. Irie, *Chem. Lett.* **2011**, *40*, 635–637.
- [10] J.-C. Micheau, C. Coudret, O. I. Kobeleva, V. A. Barachevsky, V. N. Yarovenko, S. N. Ivanov, B. V. Lichitsky, M. M. Krayushkin, *Dyes Pigm.* **2014**, *106*, 32–38.
- [11] a) W. Zhu, Y. Yang, R. Métivier, Q. Zhang, R. Guillot, Y. Xie, H. Tian, K. Nakatani, *Angew. Chem. Int. Ed.* **2011**, *50*, 10986–10990; *Angew. Chem.* **2011**, *123*, 11178–11182; b) W. Li, C. Jiao, X. Li, Y. Xie, K. Nakatani, H. Tian, W. Zhu, *Angew. Chem. Int. Ed.* **2014**, *53*, 4603–4607; c) S. Pu, C. Zheng, Q. Sun, G. Liu, C. Fan, *Chem. Commun.* **2013**, *49*, 8036–8038.
- [12] R. Göstl, B. Kobin, L. Grubert, M. Pätzelt, S. Hecht, *Chem. Eur. J.* **2012**, *18*, 14282–14285.
- [13] F. Stellacci, C. Bertarelli, F. Toscano, M. Z. Gallazi, G. Zotti, G. Zerbi, *Adv. Mater.* **1999**, *11*, 292–295.
- [14] S. Fukumoto, T. Nakashima, T. Kawai, *Angew. Chem. Int. Ed.* **2011**, *50*, 1565–1568; *Angew. Chem.* **2011**, *123*, 1603.
- [15] S. Fukumoto, T. Nakashima, T. Kawai, *Eur. J. Org. Chem.* **2011**, 5047–5053.
- [16] K. Morinaka, T. Ubukata, Y. Yokoyama, *Org. Lett.* **2009**, *11*, 3890–3893.
- [17] a) H. Utsumi, D. Nagahama, H. Nakano, Y. Shirota, *J. Mater. Chem.* **2000**, *10*, 2436–2437; b) Y. Shirota, H. Utsumi, T. Ujike, S. Yoshikawa, K. Moriwaki, D. Nagahama, H. Nakano, *Opt. Mater.* **2002**, *21*, 249–254; c) H. Utsumi, D. Nagahama, H. Nakano, Y. Shirota, *J. Mater. Chem.* **2002**, *12*, 2612–2619.
- [18] H. Kamiya, S. Yangisawa, S. Hiroto, K. Itami, H. Shinokubo, *Org. Lett.* **2011**, *13*, 6394–6397.
- [19] S. Kawai, T. Nakashima, Y. Kutsunugi, H. Nakagawa, H. Nakano, T. Kawai, *J. Mater. Chem.* **2009**, *19*, 3606–3611.
- [20] H. Nishi, T. Namari, S. Kobatake, *J. Mater. Chem.* **2011**, *21*, 17249–17258.
- [21] F. Sauter, H. Fröhlich, W. Kalt, *Synthesis* **1989**, *10*, 771–773.
- [22] K. Matsuda, K. Takayama, M. Irie, *Chem. Commun.* **2001**, 363–364.
- [23] a) J. Massaad, J.-C. Micheau, C. Coudret, R. Sanchez, G. Guirado, S. Delbaere, *Chem. Eur. J.* **2012**, *18*, 6568–6575. See also: b) S. Delbaere, J. Berthet, T. Shiozawa, Y. Yokoyama, *J. Org. Chem.* **2012**, *77*, 1853–1859; c) R. Göstl, B. Kobin, L. Grubert, M. Pätzelt, S. Hecht, *Chem. Eur. J.* **2012**, *18*, 14282–14285; d) S. Aloïse, M. Sliwa, G. Buntinx, S. Delbaere, A. Perrier, F. Maurel, D. Jacquemin, M. Takeshita, *Phys. Chem. Chem. Phys.* **2013**, *15*, 6226–6234.
- [24] a) M. Irie, T. Eriguchi, T. Takada, K. Uchida, *Tetrahedron* **1997**, *53*, 12263–12271; b) A. T. Bens, D. Frewert, K. Kodatis, C. Krysch, H.-D. Martin, H. P. Trommsdorf, *Eur. J. Org. Chem.* **1998**, 2333–2338.
- [25] Crystallographic data of **TT0**: $\text{C}_{41}\text{H}_{26}\text{F}_6\text{S}_2$, $\text{C}_{32}\text{H}_{20}\text{F}_6\text{S}_2$, $a = 9.9787(2)$ Å, $b = 11.4122(2)$ Å, $c = 15.1487(3)$ Å, $V = 1597.53(6)$ Å³, $\alpha = 70.9671(7)^\circ$, $\beta = 89.4662(7)^\circ$, $\gamma = 78.8813(7)^\circ$, $\rho_{\text{calcd.}} = 1.448$ g/cm³, triclinic. Of the 27724 reflections measured, up to $2\theta = 55.0^\circ$ were collected, 4731 were unique ($R_{\text{int}} = 0.0237$). Hydrogen atoms were calculated, in: riding positions. CCDC-987958 contains the supplementary crystallographic data for this paper. These data can be obtained free of charge from The Cambridge Crystallographic Data Centre via www.ccdc.cam.ac.uk/data_request/cif.
- [26] Crystallographic data of **BT0**: $a = 14.1418(9)$ Å, $b = 7.7792(5)$ Å, $c = 47.021(3)$ Å, $V = 5172.8(6)$ Å³, $\rho_{\text{calcd.}} = 1.496$ g/cm³, orthorhombic. Of the 67657 reflections measured up to $2\theta = 55.0^\circ$ were collected, 7323 were unique ($R_{\text{int}} = 0.1590$). CCDC-961406 contains the supplementary crystallographic data for this paper. These data can be obtained free of charge from The Cambridge Crystallographic Data Centre via www.ccdc.cam.ac.uk/data_request/cif.

- [27] a) S. Kobatake, K. Uchida, E. Tsuchida, M. Irie, *Chem. Commun.* **2002**, 2804–2805; b) M. Morimoto, M. Irie, *Chem. Commun.* **2005**, 3895–3905.
- [28] a) T. Nakashima, K. Yamamoto, Y. Kimura, T. Kawai, *Chem. Eur. J.* **2013**, *19*, 16972–16980; b) H. Suezama, T. Yoshida, Y. Umezawa, S. Tsuboyama, M. Nishio, *Eur. J. Inorg. Chem.* **2002**, 3148–3155.
- [29] A. Fihey, A. Perrier, F. Maurel, *J. Photochem. Photobiol. A* **2012**, *247*, 30–35.
- [30] In **BTo**, DFT calculations also predict a C–H bond length contraction (0.0008 Å) for the methyl involved in the noncovalent interaction with the benzothiophene unit, when compared to the carbon–hydrogen bond lengths for the two hydrogens of **TTo** (used here as a reference). This contraction is often correlated to CH– π interactions, and confirms the benzothiophene's capacity to generate the present robust CH– π bonding interaction (see A. Baggioli, S. V. Meille, G. Raos, R. Po, M. Brinkmann, A. Famulari, *Int. J. Quantum Chem.* **2013**, *113*, 2154–2162).
- [31] Ring cyclization quantum yield of **BTo** in acetonitrile, a more polar solvent, was about 0.8 ± 0.1 . A VT-NMR experiment in the same solvent afforded $84\% \pm 7\%$ population of the photo-reactive conformer, associated with a ΔG^0 (293 K) value of $1.0 \text{ kcal mol}^{-1}$, which is in good consistency with the above-mentioned ring cyclization (see the Supporting Information). One could expect that weak interactions such as H–F bonding would be weaker in a more polar solvent such as acetonitrile, and result in a decrease of the ring cyclization quantum yield. And yet, a slight increase of $\Phi_{o/c}$ was observed in acetonitrile vs. toluene. This difference might stem from a larger destabilization of the parallel conformer compared to the antiparallel one when changing the solvent polarity, while the energy barrier would remain unaffected ($\Delta G^{\text{BTo}}(\text{toluene}) < \Delta G^{\text{BTo}}(\text{acetonitrile})$).
- [32] G. Liu, S. Pu, C. Fan, S. Cui, *Dyes Pigm.* **2012**, *95*, 553–562.

Received: June 19, 2014

Published Online: ■

Published Online: ■

We provide evidence (VTNMR, X-ray data, DFT simulations) that a standard nonsymmetric diarylethene containing a benzothiophene unit achieves high ring cyclization quantum yield by means of favorable intramolecular interactions (CH- π , H-F bonding or steric hindrance).



O. Galangau, Y. Kimura, R. Kanazawa,
T. Nakashima, T. Kawai* 1–10

Enhanced Photochemical Sensitivity in
Photochromic Diarylethenes Based on a
Benzothiophene/Thiophene Nonsymmetrical Structure



Keywords: Photochromism / Noncovalent interactions / Density functional calculations / Diarylethenes